The Design of Vertical RS-CRC and LDPC Code for Ship-Based Satellite Communications On-the-Move

BINGRUI WANG[1], PINGPING CHEN [ID][2], (Member, IEEE), YI FANG [ID][3,4], (Member, IEEE), AND FRANCIS C. M. LAU [ID][5], (Senior Member, IEEE)

[1]Department of Software Technology, Nanyang Normal University, Nanyang 473061, China
[2]Department of Electronic Information, Fuzhou University, Fuzhou 350108, China
[3]School of Information Engineering, Guangdong University of Technology, Guangzhou 510006, China
[4]National Mobile Communications Research Laboratory, Southeast University, Nanjing 210096, China
[5]Department of Electronic and Information Engineering, The Hong Kong Polytechnic University, Hong Kong

Corresponding author: Pingping Chen (ppchen.xm@gmail.com)

ABSTRACT This paper investigates the decoding performance of channel-coded ship-based satellite communications on-the-move (SSCOTM) between ships and satellites. In practical communications, ship antennas deviated from satellites by wind waves suffer rapid channel degradation with serious burst errors and even losing all the data. To address this issue, we first establish a mathematical model to study the influence of wind waves and derive the effective signal-to-noise ratio (SNR) in SSCOTM. Second, we propose a vertical Reed–Solomon (RS) with cyclic redundancy check (CRC) and low-density parity check (VRC-LDPC) code, where the RS code and LDPC code are treated as the inner code and outer code to correct both burst and random errors, respectively. Moreover, both the encoder and the decoder of the proposed VRC-LDPC can be carried out in parallel implementations. Finally, simulation results show that the proposed VRC-LDPC performs much better than the conventional codes of the Consultative Committee for Space Data Systems (CCSDS) standard. Thus, this paper provides an excellent alternative channel code for reliable error-correction systems of SSCOTM.

INDEX TERMS LDPC, ship-based satellite communications, burst error.

I. INTRODUCTION

Ship-based satellite communications on-the-move (SSCOTM) can be used in various applications, such as warships exchanging reliable military information with headquarters by SSCOTM [1]. However, ships in the sea are vulnerable to wind waves, causing shaking disturbance in communications [2]. The antenna of SSCOTM may deviate seriously from that of a satellite even with minor disturbance. Thus, the received signal-to-noise ratio (SNR) is greatly degraded and a large number of burst errors occur in the received data [3]–[6]. In severe shaking disturbance, the communication between SSCOTM and the satellite is interrupted. Moreover, it is harder to achieve reliable communications for SSCOTM as transmission rate increases. To address this issue, we employ error-correction codes in SSCOTM to

ensure reliable communications [7]. However, to the best of our knowledge, there is little research on powerful error-correction codes for SSCOTM till now. Thus, this paper first investigates an error-correction code to improve the performance reliability of SSCOTM, which is of great theoretical and practical significance.

In satellite communication systems, there are mainly four types of error-correction codes, convolutional codes, Reed Solomon (RS) codes, Turbo codes, and Low Density Parity Check (LDPC) codes. The convolutional codes with Viterbi algorithm enjoy 7 dB coding gain compared with the uncoded case. Katsiotis *et al.* [8] utilized puncturing and path pruning to construct large families of convolutional codes of various code rates. The complexity of hardware implementation and power consumption of Viterbi decoder were also analyzed. Skarzynski *et al.* [9] presented an adaptive communication system for satellite communications in a low Earth orbit. The basic convolutional (2, 1, 7) code was used in Consultative

---

The associate editor coordinating the review of this manuscript and approving it for publication was Jinming Wen.

Committee for Space Data Systems (CCSDS), with connection vectors 171 (octal) and 133 (octal) [10].

RS codes are nonbinary codes with strong error correction capabilities [11]. Concatenated RS-convolutional codes find popular applications in space communications. A novel iterative soft decoding algorithm was described for the concatenated RS-convolutional code to improve decoding performance [12]. To increase the decoding speed, a graphic processing unit (GPU)-accelerated decoding system was proposed for decoding massive compressed images from the satellite [13]. Zhang *et al.* [14] presented an area-efficient pipeline-balancing RS decoder for satellite communications. A new local data-link layer protocol was stated in [15], which integrated RS erasure coding to licklider transmission protocol (LTP) for more efficient data delivery. The Digital Video Broadcasting Satellite (DVB-S) exploited a concatenated coding system based on an RS (204, 188) code and a convolutional code [16]. The CCSDS adopted RS (255, 239) codes and RS (255, 223) codes as the space channel coding standard.

Turbo codes were proved to perform close to the Shannon limit [17]. Progressive channel coding methods were presented for short message transmission via satellite transponder [18]. Due to on-board resource limitation and the throughput requirements, a partial iterative decoder for on-board application was put forward with the reduced number of decoding iteration [19]. Simulation results showed that the proposed decoder greatly reduces the complexity of on-board processing without losing decoding performance. In particular, Turbo product codes (TPCs) were employed to improve the performance of satellite communication systems [20]. The CCSDS put forth several types of Turbo codes with various code lengths and coding rates [10].

An LDPC code is a linear block error-correction code and can approach the limit of Shannon capacity [21], [22]. Costantini *et al.* [23] compared the performance of protograph-based non-binary LDPC codes with that of binary LDPC and turbo codes in space communication standards. The non-binary codes outperformed the binary counterpart by more than 0.3 dB in AWGN channels, and this gain was increased to 1 dB for the short block length in CCSDS up-link standard. To reduce decoding complexity, a real-time implementation of LDPC decoder was proposed by using a lookup table in satellite communications [24]. The implementation results on Xilinx Field Programmable Gate Array (FPGA) chip illustrated that the simplified decoder can achieve at last 28.6% and 8% cost reduction in RAM and slices, respectively as compared to conventional structures. With respect to space tele-commanding standard, an ordered statistics decoder for short LDPC codes enabled significant gains over conventional iterative algorithms [25]. The CCSDS standard contained two kinds of LDPC codes, one near-space code and nine deep-space codes. The near-space LDPC code was an LDPC (8176, 7154) code with a quasi-cyclic (QC) structure. In addition, DVB-S Second Generation (DVB-S2) standard employed a concatenated

Bose-Chaudhuri-Hocquenghem (BCH)-LDPC code [26]. China developed its own Advanced Broadcasting System of Satellite (ABS-S) standard, which adopted the LDPC codes with a fixed code length of 15360 bits [27], [28].

Although the above four types of error-correction codes have their own advantages in satellite communications, they are not the best choices for SSCOTM to satisfy the demand of high-speed and reliable communications. The reasons are as follows:

1) Convolutional codes perform inferior to Turbo codes and LDPC codes in terms of correcting burst errors. Convolutional codes need to puncture bits to attain high code rates, losing some useful information. The encoding of convolutional codes is simple whereas the decoding is complex.

2) RS codes are not good at correcting random errors as compared to Turbo codes and LDPC codes, while RS codes perform well in correcting burst errors with non-binary algebraic structures. In general, an RS code with more parity-check symbols leads to better burst-error-correcting capability and larger complexity [29]. Designing an RS code with strong error-correction capability and low complexity is still a big challenge.

3) Turbo codes are hard to implement for parallel decoding while they have excellent decoding performance. Turbo codes suffer from relatively high decoding latency and decoding complexity since they adopt interleaving structures and iterative decoding algorithms. Besides, Turbo codes have relatively performance error floor.

4) LDPC codes have superior error-correction capacity and low error floor. LDPC codes also benefit from simple encoder/decoder implementations. LDPC codes perform much better than Turbo codes, RS codes and convolutional codes in correcting random errors. The near-space LDPC code given by CCSDS standard is not a full-rank matrix. The LDPC codes under DVB-S2 standard have long codewords which lead to high decoding complexity and latency.

We can see from the above analysis that these conventional codes are mainly studied to correct random errors. However, in SSCOTM systems, the most destructive factor is burst errors. Correcting burst errors is a challenge in the channel coded ship communication. However, so far little work has been reported on error-correction codes for SSCOTM communications. Thus, to achieve communications of low-latency and high reliability, this paper aims to design a good error-correction code with short codeword length for SSCOTM. Note that the satellites are nearly 36,000 kilometers away from SSCOTM and this distance belongs to near-space [30].

The rest of the paper is organized as follows. Section II gives SSCOTM communications and mainly describes how wind waves affect SSCOTM. Section III reviews conventional channel codes, and then proposes a class of
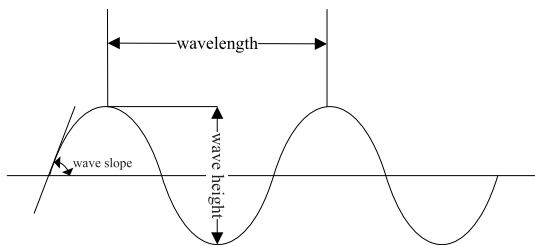
FIGURE 1. The sea wave with the related parameters.

error-correction codes for SSCOTM. Section IV shows the simulation results. Section V gives the conclusion.

II. ANALYSIS OF WIND WAVES IMPACTING ON THE SSCOTM

A. WIND WAVES IMPACTING ON THE ROLL MOTION

The communication between SSCOTM and a satellite suffers from various interference factors, such as wind wave, multipath effect, rain attenuation and sun exposure [31]. The wind wave is a major impairment for SSCOTM communications. We assume that SSCOTM is fixed on ships and study the motion of SSCOTM without other physical techniques to mitigate the offset. In other words, SSCOTM moves in the same way as ships.

Waves can be modeled by a simple function called regular waves, which are the basic objects to study wave motion. The irregular wave of the sea can be represented by summing a large number of regular sinusoidal waves. Fig. 1 shows the model of regular waves. To specify a regular wave, we need the following parameters:

- Wavelength L, the horizontal distance between two adjacent peaks or troughs.
- Wave height H, the vertical distance between the highest point and lowest point.
- Wave slope α, the angle between the tangent line and the horizontal line at a certain point on the wave surface, indicating the inclination of the wave.
- Wave period T_w, the time it takes a wave crest to travel one wavelength.

A ship at sea moves in six degrees of motions, three rotational motions and three translational motions, as shown in Fig. 2. The motions are defined as movements of the center G of ship gravity. The three rotational motions are roll, pitch and yaw around the transverse X-axis, longitudinal Y-axis and vertical Z-axis, respectively. The three translational motions are surge, sway and heave along X-axis, Y-axis and Z-axis, respectively. Of these six motions, rolling is the most significant one with regard to ship motions [32]. The main parameters of rolling are roll amplitude θ and natural roll period T_r. Rolling motion consists of two parts, free oscillation in still water and forced oscillation in period of waves. The free oscillation dies out in time by damping, leaving only the forced oscillation. The forced oscillation of ship in waves can be expressed by [33], [34]

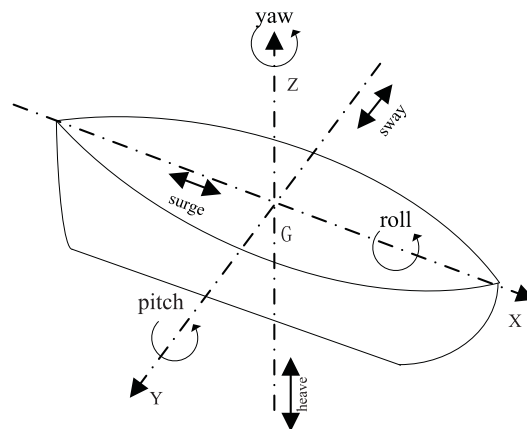$$\theta = \frac{\alpha_{max}}{1 - \left(\frac{T_r}{T_w}\right)^2}, \tag{1}$$

FIGURE 2. Ship motions in waves.

where α_{max} is the maximum wave slope, $\alpha_{max} = \frac{\pi H}{L}$, $T_w = 0.8\sqrt{L}$, and radian is the unit of amplitude θ.

The amplitude θ is positive and the ship rolls with the wave for $T_w > T_r$ while the amplitude θ is negative and the ship rolls into the wave for $T_w < T_r$, and θ is large for $T_w \approx T_r$. T_r is given as [35]

$$T_r = \frac{2.3\pi k}{\sqrt{g \cdot GM}}, \tag{2}$$

where g is the gravitational constant, GM is metacentric height, k is the roll radius of gyration, $k = 0.39 B$, and the vertical distance between the center of gravity and metacenter equals to 0.07 B where B is the breadth of ship.

To compute θ, we need to obtain wave height H and wave period T_w as in (1). The Pierson-Moskowitz formula is often used to specify H and T_w of wind waves as [36]

$$H = 2.24 \times 10^{-2}U_{10}^2, \tag{3}$$
$$T_w = 7.5 \times 10^{-1}U_{10}^2, \tag{4}$$

where U_{10} is the wind speed at a height of 10 m above the sea surface. Based on (1)–(4), the relation between roll amplitude and wind waves can be given by

$$\theta = \frac{258U_{10}^2}{56.3U_{10}^2 - 1156B}. \tag{5}$$

In addition, we can get the wind speed in terms of Beaufort numbers. Thus, the roll amplitude of ship and SSCOTM affected by wind waves can be obtained.

B. ANTENNA POINTING LOSS INTRODUCED BY ROLL MOTION

A major component of SSCOTM systems is the antenna. An important characteristic of antenna is the radiation pattern, which represents the distribution of energy transmitted or received. The radiation pattern consists of main lobes and side lobes. A main lobe has the greatest radiation intensity. The lobes except the main lobe are referred to as side lobes, which cannot be completely eliminated. We aim to minimize side lobes and improve the main lobe. H alf-power beam

width (HPBW) is a major parameter associated with the main lobe, defined by the angle between two points in the main lobe that are down from the maximum gain by 3 dB. Antennas with great HPBW typically have low gains and antennas with small HPBW tend to have higher gains. Thus, a large HPBW is often not desired. The HPBW (in degrees) is approximately given by [37]

$$\theta_{1/2} = 65\frac{\lambda}{d}, \tag{6}$$

where d is the antenna diameter, and λ is the wavelength in free space. The HPBW becomes narrow and the antenna is not easy to align as d is increased or λ is reduced.
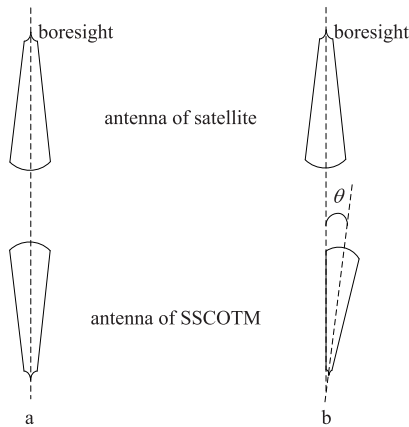

FIGURE 3. Antenna alignment and misalignment. (a) Alignment. (b) Misalignment.

Antenna alignment is vital in communications. Fig. 3.a illustrates the ideal antenna alignment when the communication between SSCOTM and a satellite is established,. In this case, the signal is received at the peak of the antenna beam of transmitted signal, and the maximum antenna gain is achieved. However, when the SSCOTM adopts Ku-band, its corresponding antenna main lobe is narrow. Thus, aligning the antenna of SSCOTM with that of a satellite is difficult [38], [39]. In addition, the SSCOTM moves in roll motion due to wind waves. The antennas cannot be targeted exactly and an antenna pointing deviation is unavoidable. Fig. 3.b shows the antenna misalignment. θ is the angle off boresight introduced by roll motion. Even a minor θ can reduce antenna gain rapidly and then many useful signal bits are lost. If the pointing deviation is severe, the communication is greatly degraded. The antenna pointing loss L_θ (dB) can be expressed as a function of θ [37]

$$L_\theta = 12\Big(\frac{\theta}{\theta_{1/2}}\Big)^2 = 12\Big(\frac{\theta d}{65\lambda}\Big)^2. \tag{7}$$

The equation (7) is valid only for small angles, $0 \le \theta \le \theta_{1/2}/2$. When θ is bigger than $\theta_{1/2}$, the boresight of satellite points to the first side lobe of that of SSCOTM. The first side lobe is adjacent to the main lobe. Referring to [40], L_θ is at least 13dB in this case. In particular, when θ continues to increase, the antenna gain is approximately zero because no useful signal can be received.

C. THE RECEIVED E_B/N_0 OF SSCOTM

The received carrier power of SSCOTM is given by

$$C = EIRP + PG - L_p - L_\theta - L_o, \tag{8}$$

where *EIRP* is the equivalent isotropic radiated power of the satellite, *PG* is the isotropic power gain of the receiving antenna, L_p is the free space path loss incurred by electromagnetic waves propagating in a straight line through space, and L_o represents other losses, such as rain attenuation loss, atmospheric absorption loss and receiver feeder loss. The free space path loss L_p is expressed as

$$L_p = 20\log_{10}\Big(\frac{4\pi r}{\lambda}\Big), \tag{9}$$

where r is the distance between SSCOTM and a satellite. The received E_b/N_0 (dB) in SSCOTM is then given by

$$\frac{E_b}{N_0} = \frac{C}{N_0 R_b}, \tag{10}$$

where R_b denotes the bit rate, E_b is the bit energy, $N_0 = k_b T$ with T being the noise temperature, and k_b is Boltzmanns constant.

Combining (5)–(7), the relation between E_b/N_0 of SSCOTM and wind waves is

$$\begin{aligned}
\frac{E_b}{N_0} &= \frac{C}{N_0 R_b} \\
&= \frac{1}{N_0 R_b}(EIRP + PG - L_p - L_\theta - L_o) \\
&= \frac{1}{N_0 R_b}\Big(EIRP + PG - L_p - 12\Big(\frac{\theta d}{65\lambda}\Big)^2 - L_o\Big) \\
&= \frac{1}{N_0 R_b}\Big(EIRP + PG - L_p \\
&\quad - 12\Big(\frac{3.97 U_{10}^2 d}{(56.3 U_{10}^2 - 1156B)\lambda}\Big)^2 - L_o\Big).
\end{aligned} \tag{11}$$

III. THE PROPOSED ERROR-CORRECTION CODE

Recall that burst errors play a critical role in degrading the performance of SSCOTM. Especially when the antenna of SSCOTM largely deviates from that of a satellite, burst errors occur in the communication. In this section, we show the simulated performance of the CCSDS codes, i.e., convolutional codes, RS codes, Turbo codes and LDPC codes over the channels with burst errors. Then we propose a powerful code for SSCOTM.

A. BURST ERROR-CORRECTION CAPABILITIES OF TRADITIONAL CODES

First, we consider CCSDS convolutional (2000, 1000) code. Fig. 4 plots the bit error rate (BER) curve vs the length of burst error when employing Viterbi soft decoding. We can see that when the burst errors with a length less than 10 bits can be corrected. As burst length increases, the convolutional code fails to correct the errors. The burst-error-correction capacity of the convolutional code is relatively limited.

Second, it is known that RS (n, k) codes can correct $t = (n - k)/2$ symbol errors. A symbol has w bits. We test the
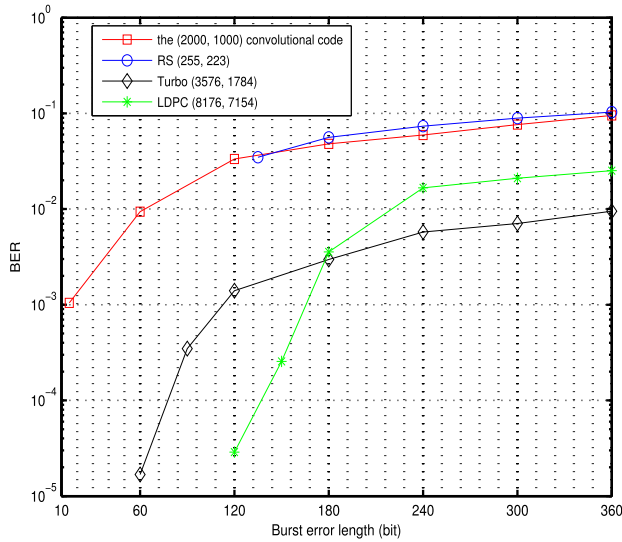
FIGURE 4. BER vs burst error length of the convolutional code, RS (255, 223), Turbo (3576, 1784) and LDPC (8176, 7154).

RS (255, 223) code which has more parity bits than RS (255, 239) in CCSDS standard. In theory, the RS (255, 223) code can correct 128 error bits. Fig. 4 shows that the RS code cannot correct burst errors more than 128 bits.

Third, we simulate the CCSDS Turbo (3576, 1784) code at the code rate of 1/2 by soft output Viterbi algorithm decoding with 12 iterations. We can see from Fig. 4, the performance is greatly degraded when the length of burst error exceeds 80 bits.

Finally, with regard to an LDPC (8176, 7154) code, Fig. 4 depicts the simulation result by using belief propagation decoding with 12 iterations. If the length of burst error is 120, the BER achieves 10^{-5}. In contrast, no matter how severe burst errors are, RS codes can correct the errors if they are no more than half of parity bits.

By comparing the simulation result in Fig. 4, we employ the RS code to correct burst errors due to its good performance and determined burst-error-correction capacity. Moreover, we choose LDPC code to correct random errors induced by channel noise since the LDPC code performs best in correcting random errors among the four CCSDS codes.

B. THE STRUCTURE OF VERTICAL RS-CRC

We often use Cyclic Redundancy Check (CRC) codes to detect the errors first before error correction. CRC codes are easy to implement and detect burst/random errors efficiently. In this section, we propose a vertical RS-CRC and LDPC (VRC-LDPC) code where the RS code and LDPC code are treated as the inner code and the outer code, respectively. Due to the advantages of CRC, RS and LDPC codes, we can detect and correct burst and random errors. We elaborate the proposed VRC code in the following parts.

The RS codes can correct t burst symbol errors, i.e., tw burst bit errors. Moreover, by using erasure decoding, RS codes can correct $2tw$ burst errors [41]. The erasure

decoding requires other error control codes to provide erasure information. The VRC code consists of two component codes, CRC codes and RS (n_5, k_5) codes. The encoding and decoding of VRC are introduced as below.

The VRC encoding consists of the following steps:

- Step 1. A set of $a_1 a_2 - 1$ message symbols is arranged in an $a_1 \times a_2$ array with one empty position, which is in the uth column for CRC check symbol, as shown in Fig. 5. When a_2 is an odd number, $u = (a_2 - 1)/2 + 1$, and when a_2 is an even number, $u = a_2/2$.
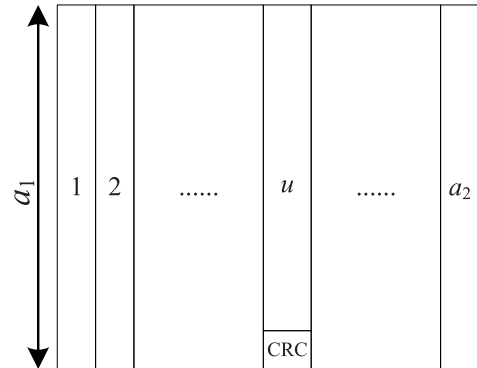

FIGURE 5. The plane structure of VRC.

- Step 2. Apply a CRC (p, q) coding to the $a_1 a_2 - 1$ symbols. We can generate a CRC check symbol at the empty position in the uth column. The check symbol has w bits, $p = (a_1 a_2)w$ and $q = (a_1 a_2 - 1)w$.
- Step 3. Repeat steps 1) and 2) for k_5 times and vertically stack the k_5 planes to form an $a_1 \times a_2 \times k_5$ array. This process is illustrated as the top k_5 layers in Fig. 6.
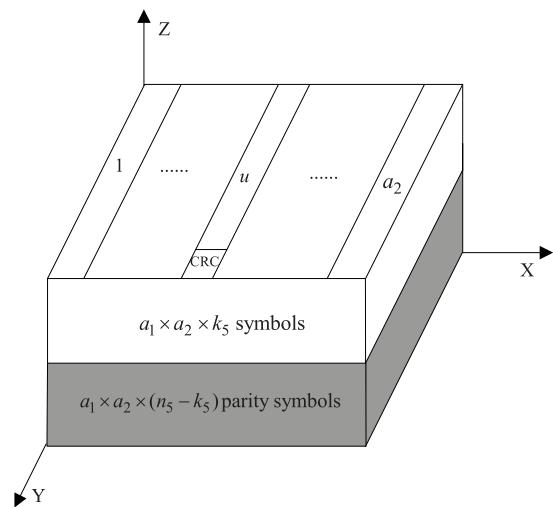

FIGURE 6. The whole structure of VRC.

- Step 4. In the Z-axis direction, apply RS (n_5, k_5) encoding to each sequence of the $a_1 \times a_2 \times k_5$ array. Therefore, with the generated ($n_5 - k_5$) parity symbols in each sequence, an $a_1 \times a_2 \times n_5$ array is formed. The bottom gray parts in Fig. 6 are the parity symbols.

Note that the lengths of a_1, a_2 and n_5 are small. Thus, we can apply the RS (n_5, k_5) encoding simultaneously to all $a_1 \times a_2$ sequences in step 4. Then, the encoded data can be transmitted layer by layer. Finally, the proposed VRC code can be denoted by VRC (n_5, k_5, a_1, a_2, w).

The VRC decoding is described as follows:

- The received data are stored in an $a_1 \times a_2 \times n_5$ array as shown in Fig. 6.
- Apply CRC error detecting simultaneously to the top k_5 layers of $a_1 \times a_2 \times n_5$ array. If the CRC check does not agree with one layer, we say that the layer is corrupted by errors. Moreover, if many consecutive layers fail to agree with the CRC check, it suggests that lots of data of the layers are damaged by burst errors. The layers are flagged as erasure information, which declare the locations of burst errors.
- Employ RS (n_5, k_5) erasure decoding simultaneously to all sequences of $a_1 \times a_2 \times n_5$ array with the erasure information provided by the layers.

C. THE PROPOSED LDPC

In the proposed VRC-LDPC, we adopt Quasi-Cyclic LDPC (QC-LDPC) code as a component code for its simple hardware implementation. The parity-check matrix of a QC-LDPC (n, k) code is given by

$$H = \begin{bmatrix} A_{1,1} & A_{1,2} & \cdots & A_{1,j} \\ A_{2,1} & A_{2,2} & \cdots & A_{2,j} \\ \vdots & \vdots & \ddots & \vdots \\ A_{i,1} & A_{i,2} & \cdots & A_{i,j} \end{bmatrix}. \quad (12)$$

Each $A_{i,j}$ is a $sx \times sx$ square matrix that is a right cyclic shift of its preceding row. The structure of $A_{i,j}$ is determined by the position of 1's in the first row, $j \cdot sx = n$ and $i \cdot sx = n - k$. Next, we discuss the general encoding algorithm for LDPC codes. Let the matrix H be expressed as $\begin{bmatrix} H^p & H^m \end{bmatrix}$ and generator matrix G as $\begin{bmatrix} B & I \end{bmatrix}$. The sizes of H^p, H^m, B and I are $(n-k) \times (n-k), (n-k) \times k, k \times (n-k)$ and $k \times k$, respectively. The relation between the H and G can be given by

$$HG^T = \begin{bmatrix} H^p & H^m \end{bmatrix} \begin{bmatrix} B^T \\ I \end{bmatrix} = H^p B^T + H^m I = 0. \quad (13)$$

Then, the B can be written as

$$B = \left[(H^p)^{-1} H^m I \right]^T. \quad (14)$$

Let M be the message with length k. Then we can obtain a codeword $C = M \cdot G$. If H^p is singular, G is not easy to achieve. In fact, H of CCSDS LDPC (8176, 7154) code is not a full-rank matrix. The H consists of a 2×16 array of 511×511 square circulants, and H^p is

$$H^p = \begin{bmatrix} A_{1,1} & A_{1,2} \\ A_{2,1} & A_{2,2} \end{bmatrix}, \quad (15)$$

and H^m be

$$H^m = \begin{bmatrix} A_{1,3} & A_{1,4} & \cdots & A_{1,16} \\ A_{2,3} & A_{2,4} & \cdots & A_{2,16} \end{bmatrix}. \quad (16)$$

In this case, H^p is not full rank and then the inverse matrix of H^p can not obtained since the 511th and the 1022th columns are relevant. To ensure H^p to be full rank and QC structured, we substitute two identity matrices for $A_{1,1}$ and $A_{2,2}$ without generating girth–4 cycles. Thus, the resulting H^p has inverse matrix, which can be encoded with the general encoding algorithm. Moreover, to achieve the high-speed satellite comminations, we next construct a short LDPC code.

In QC-LDPC codes, Malema [42] proposed an algorithm to construct short codes with girth 8 to achieve excellent decoding performance. However, the parity-check matrix of Malema's construction is singular and it is not hardware-friendly. Thus, we propose fast full-rank (LDPC-F) and slow full-rank (LDPC-S) algorithms to transform the singular matrix H^p to be full rank. With (12) and (13), H^p can be written as

$$H^p = \begin{bmatrix} A_{1,1} & A_{1,2} & \cdots & A_{1,i} \\ A_{2,1} & A_{2,2} & \cdots & A_{2,i} \\ \vdots & \vdots & \ddots & \vdots \\ A_{i,1} & A_{i,2} & \cdots & A_{i,i} \end{bmatrix}. \quad (17)$$

Define Z as an all zeros square $sx \times sx$ matrix. The LDPC-F algorithm is given as below:

- Step 1. Substitute Z for all diagonal matrices, $A_{1,1}, A_{2,2}, \cdots, A_{i,i}$.
- Step 2. If step 1 fails to make H^p full rank, then replace an $A_{i,1}$ of the first column with Z, and replace an $A_{j,c}$ ($c \le i, j \ne i$) with Z, but keep no two Z in the same row or the same column. At one time, the number of replaced A matrices is i. The number for possible replacements is $i \cdot (i-1) \cdots 2 \cdot 1$.

After the two steps, the H^p can become a full-rank matrix. The LDPC-F algorithm does not add extra 1 to H^p which means no girth less than 8 is generated. Thus, based on Malema's construction and LDPC-F algorithm, we can obtain a nonsingular LDPC (4000, 3250) code with girth 8.

The LDPC-S algorithm is expressed as follow:

- Step 1. Define $E_1, E_2, \cdots, E_i$ as square matrices with size $sx \times sx$, and the positions of 1's in first rows of E_1, $E_2, \cdots, E_i$ are 1.
- Step 2. Let $E_1, E_2, \cdots, E_i$ be cyclic matrices. Substitute $E_1, E_2, \cdots, E_i$ for $A_{1,1}, A_{2,2}, \cdots, A_{i,i}$. If the H^p is nonsingular and has no 4 girth, the procedure stops.
- Step 3. Change the number of 1's positions in first rows of $E_1, E_2, \cdots, E_i$ from 2 to o, $o \le i$.
- Step 4. For each change, if step 2 is satisfied, then stop the algorithm, and go to step 3 otherwise.

In general, a nonsingular H^p can be obtained when $o \le 5$. Usually, we only need to replace $A_{2,2}$ and $A_{3,3}$ with E_2 and E_3. Actually, we can obtain a full-rank LDPC (4000, 3250) code with girth 6 by using LDPC-S.

Given the proposed full-rank codes, we construct a VRC-LDPC code. As shown in Fig. 7, we first apply (n_5, k_5, a_1, a_2, w) VRC encoding, and $a_1 a_2 (n_5 - k_5) w$ parity
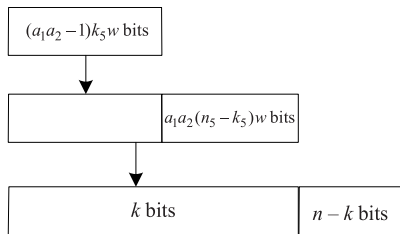
FIGURE 7. The structure of VRC-LDPC.

bits are appended to the end of $a_1(a_2 - 1)k_5w$ information bits. A symbol has w bits. Then, we generate a codeword of length n bits by the LDPC encoding with $n-k$ parity bits, $k = a_1a_2n_5w$. The SSCOTM can adopt the VRC-LDPC code that consists of an (n_5, k_5, a_1, a_2, w) VRC and a QC LDPC. Note that in this paper, we use the VRC-LDPC code consisting of VRC (26, 20, 5, 5, 5) and LDPC (4000, 3250). The code rate of this VRC-LDPC is $\frac{20(5\times5-1)}{(5\times5\times26)} \cdot \frac{3250}{4000} = 0.6$.

IV. THE EXPERIMENT RESULTS

The SSCOTM operates at Ku band with the typical parameters illustrated in Table 1. From (6), we can see that the corresponding HPBW $\theta_{1/2} \approx 1.3$ degree. Given the parameters, we conduct the performance simulation of the VRC-LDPC code in this scenario.

TABLE 1. The parameters in detail.

parameter	value
PG	41.1 dB
r	35,786,000 m
f	12.5 GHz
d	1.2 m
L_o	4 dB
T	293 K
k_b	1.38×10^{-23} J/K
B	20 m

A. BURST ERROR CORRECTING PERFORMANCE

The VRC-LDPC code utilizes a VRC code to correct burst errors. In the SSCOTM communications, we consider that the top $n_5 - k_5$ consecutive layers of the received $a_1 \times a_2 \times n_5$ data array are corrupted by burst errors. We next analyze the error-correct capacity of the VRC-LDPC code.

Note that burst errors can occur in every part of the $a_1 \times a_2 \times n_5$ data array. The red parts in Fig. 8 illustrate the data destroyed by burst errors. We perform VRC decoding. First, apply CRC decoding to each layer. If the $n_5 - k_5$ layers do not agree with CRC check, it means that burst errors interfere with the layers. Second, the $n_5 - k_5$ layers are marked as erasure information. Third, the $(n_5 - k_5)$ errors within erasure-correction capability of RS (n_5, k_5) can be corrected by using the erasure decoding. Thus, we can recover all the data due to the protection from VRC code. The RS (n_5, k_5) can correct up to $(n_5 - k_5)$ burst errors, but fails to correct more errors. The maximum number of correctable burst errors of VRC codes is $a_1a_2(n_5 - k_5)w$ bits. Note that if the number of burst errors
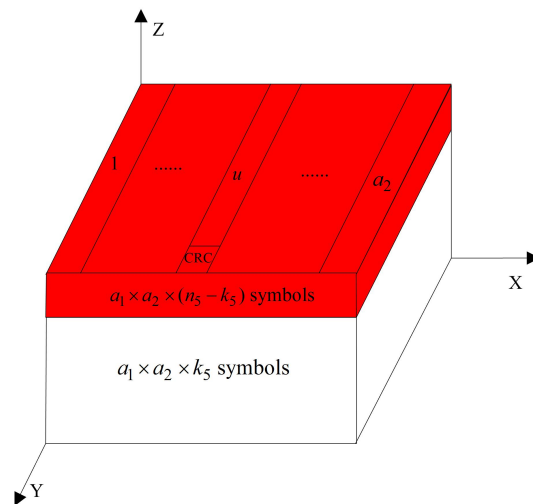

FIGURE 8. Data corrupted by burst errors.

in other parts of data array is shorter than $(n_5 - k_5)$ layers, the errors can also be corrected.

In the SSCOTM communications, with ship breadth of 20 m and $U_{10} \geq 8$m/s, the off-boresight angle θ is bigger than 0.85 degrees according to (5). In this case, the θ is bigger than $\theta_{1/2} = 0.65$ degrees and the main lobe of antenna of SSCOTM deviates from that of a satellite. Seeing (7) and (11), when R_b is bigger than 25 Mb/s, the E_b/N_0 decreases rapidly to zero or even a negative value. The burst errors occur in this scenario, and we use the VRC-LDPC code consisting of VRC (26, 20, 5, 5, 5) and LDPC (4000, 3250). Fig. 9 shows the curve of E_b/N_0 of VRC-LDPC versus the length of burst errors. We can see that burst errors less than 750 bits can be fully corrected by the VRC-LDPC.
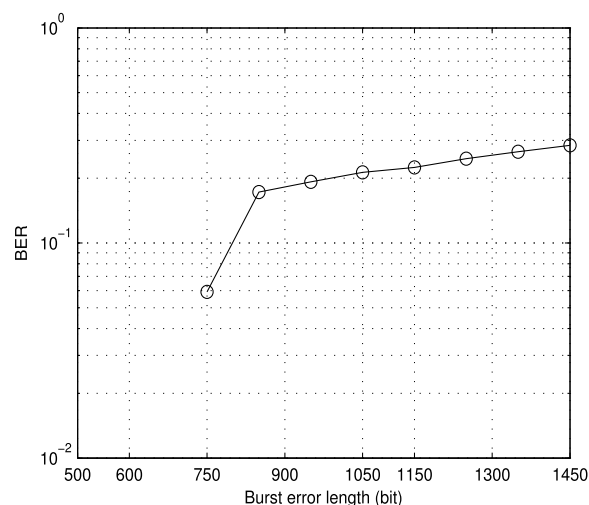

FIGURE 9. BER vs burst error length of VRC-LDPC.

B. RANDOM ERROR CORRECTING PERFORMANCE

Recall that SSCOTM is corrupted by both burst errors and random errors. We can exploit the LDPC code in the

VRC-LDPC code to correct random errors. The LDPC (4000, 3250) code can be constructed by fast and slow full-rank algorithms as LDPC-F and LDPC-S, respectively.
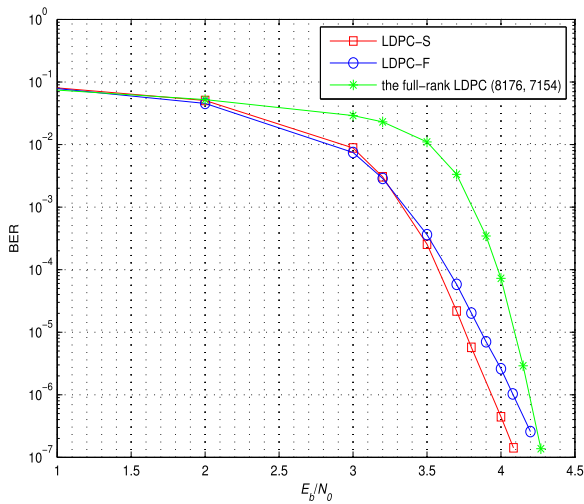

FIGURE 10. The performance of three LDPC codes in SSCOTM communications.

Using the min-sum decoding with 8 iterations, Fig. 10 compares the decoding performance of the full-rank CCSDS LDPC (8176, 7154) code, and the codes constructed by LDPC-F and LDPC-S. We can see that all the codes have no error floor above BER 10^{-7}. The LDPC-F code performs worse than LDPC-S one. It is because some cyclic matrices are replaced with all zero matrices in LDPC-F, eliminating useful connection. The LDPC-S code achieves performance gains of 0.5 dB and 0.2 dB over the LDPC (8176, 7154) code at the BER of 10^{-4} and 10^{-7}, respectively. In addition, the LDPC-S has lower complexity and decoding delay for its short length less than half length of the LDPC (8176, 7154). Thus, the LDPC-S is the best choice in the VRC-LDPC code among the three codes.

To verify the advantage of the VRC-LDPC, Fig. 11 compares the BER performance of the VRC-LDPC, the convolutional (4000, 2000) code [10], and TPC (3965, 2401) code [20] in SSCOTM communications. The TPC code consists of the shortened TPC (61, 49) code and TPC (65, 49) code. The three codes have almost the same codeword length 4000 bits. The code rate of the VRC-LDPC and the TPC code is 0.6, while the rate of the convolutional code is 0.5. The VRC-LDPC, the TPC code and the convolutional code employ min-sum decoding, Chase decoding and Viterbi decoding, respectively.

We can see that the VRC-LDPC code outperforms both the TPC code and the convolutional code when BER is below 10^{-4}, while the convolutional code performs better than the VRC-LDPC and the TPC code at low E_b/N_0 regime. In particular, from (11), we can see that the E_b/N_0 increases as U_{10} decreases. For $U_{10} = 7.26$ m/s and $R_b = 75$ Mb/s, the corresponding E_b/N_0 is approximately 3.7 dB. In this point, the VRC-LDPC achieves gains of 0.1 dB and 1.3 dB
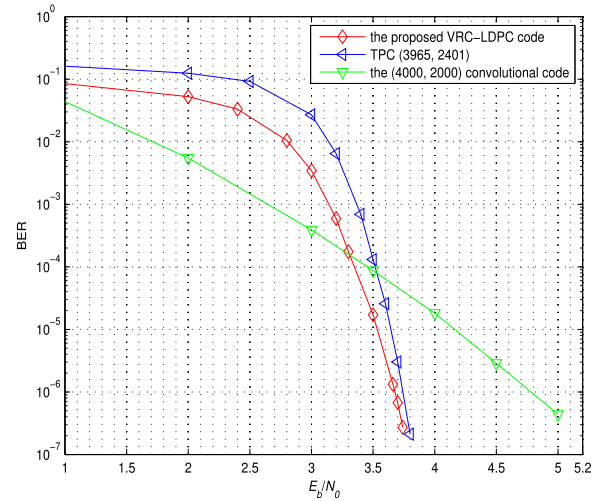

FIGURE 11. The performance of VRC-LDPC, TPC code and the convolutional code in SSCOTM communications.

over the TPC code and the convolutional code at the BER of 10^{-7}, respectively. Thus, the performance advantage of the proposed VRC-LDPC is demonstrated. Moreover, Fig. 12 shows that the convolutional code and the TPC code can correct burst errors about 20 bits. Recall that the correctable burst error length of the VRC-LDPC is 750 bits in Fig. 9, which is 37 times larger than that of the two other codes.
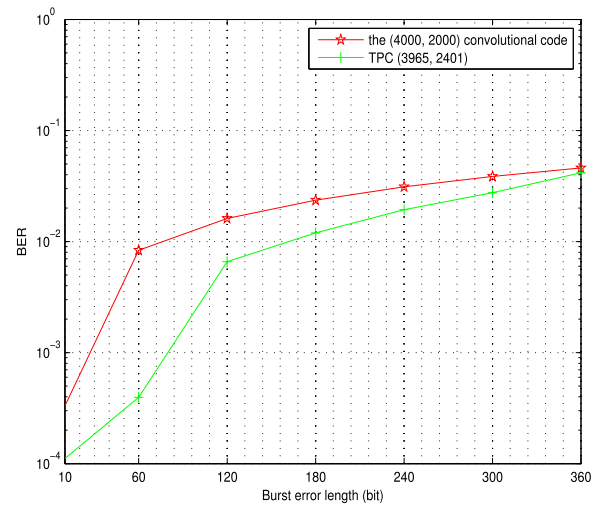

FIGURE 12. BER vs burst error length of the convolutional code and the TPC code.

V. CONCLUSION

This paper presents a VRC-LDPC code to correct burst errors and random errors in the communication between SSCOTM and a satellite. The VRC-LDPC code consists of RS-based VRC code and LDPC code. The proposed code enables simple hardware implementation by using the simplified min-sum decoding. In addition, the proposed code has lower decoding latency as compared to the conventional CCSDS LDPC code for its parallel implementation and the shorter

code length. To validate the proposed code, we conduct detailed analysis and experiments. The proposed VRC-LDPC is proved to correct the maximum burst errors up to 750 bits, which is better than the conventional CCSDS convolutional code and TPC code. In particular, the proposed VRC-LDPC code achieves excellent performance and has no error floor at the BER of 10^{-7}. Thus, the VRC-LDPC code effectively corrects both burst and random errors, which serves as a first foray into the investigation of channel coding for SSCOTM systems.

REFERENCES

[1] R. Santamarta, "SATCOM terminals: Hacking by air, sea, and land," IOActive Inc., Seattle, WA, USA, White Paper 1, 2014.

[2] C. Heij and S. Knapp, "Effects of wind strength and wave height on ship incident risk: Regional trends and seasonality," *Transp. Res. D, Transp. Environ.*, vol. 37, pp. 29–39, Jun. 2015.

[3] V. Weerackody and E. G. Cuevas, "Technical challenges and performance of satellite communications on-the-move systems," *Johns Hopkins APL Tech. Dig.*, vol. 30, no. 2, pp. 113–121, 2011.

[4] V. Weerackody and L. Gonzalez, "Mobile small aperture satellite terminals for military communications," *IEEE Commun. Mag.*, vol. 45, no. 10, pp. 70–75, Oct. 2007.

[5] J. Wen, L. He, and F. Zhu, "Swarm robotics control and communications: Imminent challenges for next generation smart logistics," *IEEE Commun. Mag.*, vol. 56, no. 7, pp. 102–107, Jul. 2018.

[6] J. Wen, K. Wu, C. Tellambura, and P. Fan, "A closed-form symbol error rate analysis for successive interference cancellation decoders," *IEEE Trans. Wireless Commun.*, to be published.

[7] D. Roddy, *Satellite Communications* Two Penn Plaza, NY, USA: McGraw-Hill, 2006, pp. 315–324.

[8] A. Katsiotis, P. Rizomiliotis, and N. Kalouptsidis, "Flexible convolutional codes: Variable rate and complexity," *IEEE Trans. Commun.*, vol. 60, no. 3, pp. 608–613, Mar. 2012.

[9] J. Skarzynski, M. Darmetko, S. Kozlowski, and K. Kurek, "SDR implementation of the receiver of adaptive communication system," *Radio Sci.*, vol. 51, no. 4, pp. 344–351, Apr. 2016.

[10] *TM Synchronization and Channel Coding. Recommendation for Space Data System Standards*, document CCSDS 131.0-B-3, Sep. 2017.

[11] I. S. Reed and G. Solomon, "Polynomial codes over certain finite fields," *J. Soc. Ind. Appl. Math.*, vol. 8, no. 2, pp. 300–304, Jun. 1960.

[12] C. Li, "Iterative soft decoding of Reed-Solomon convolutional concatenated Codes," *IEEE Trans. Commun.*, vol. 61, no. 10, pp. 4076–4085, Oct. 2013.

[13] C. Song, Y. Li, and B. Huang, "A GPU-accelerated wavelet decompression system with SPIHT and Reed-Solomon decoding for satellite images," *IEEE J. Sel. Topics Appl. Earth Observ. Remote Sens.*, vol. 4, no. 3, pp. 683–690, Sep. 2011.

[14] B. Zhang, H. Liu, and X. Yang, "Area-efficient Reed-Solomon decoder for 10 Gbps satellite communication," *IEICE Electron. Expr.*, vol. 8, no. 13, pp. 1001–1007, 2011.

[15] L. Shi *et al.*, "Integration of Reed-Solomon codes to licklider transmission protocol (LTP) for space DTN," *IEEE Aerosp. Electron. Syst. Mag.*, vol. 32, no. 4, pp. 48–55, Apr. 2017.

[16] *Channel Coding and Modulation for 11/12 GHz Satellite Services*, European Standard EN 300 421 V1.1.2, Aug. 1997.

[17] C. Berrou and A. Glavieux, "Near optimum error correcting coding and decoding: Turbo-codes," *IEEE Trans. Commun.*, vol. 44, no. 10, pp. 1261–1271, Oct. 1996.

[18] J. Rumanek, and J. Šebesta, "New channel coding methods for satellite communication," *Radioengineering*, vol. 19, no. 1, pp. 155–161, Apr. 2010.

[19] L. Hang, G. Zhen, Z. Ming, and W. Jing, "Partial iterative decode of turbo codes for on-board processing satellite platform," *China Commun.*, vol. 12, no. 11, pp. 1–8, Nov. 2015.

[20] H. Mukhtar, A. Al-Dweik, and A. Shami, "Turbo product codes: Applications, challenges, and future directions," *IEEE Commun. Surveys Tuts.*, vol. 18, no. 4, pp. 3052–3069, Apr. Apr. 2016.

[21] R. G. Gallager, "Low-density parity-check codes," *IRE Trans. Inf. Theory*, vol. 8, no. 1, pp. 97–104, Jan. 1962.

[22] D. J. C. MacKay and R. M. Neal, "Near Shannon limit performance of low-density parity-check codes," *Electron. Lett.*, vol. 32, pp. 1645–1646, Aug. 1996.

[23] L. Costantini, B. Matuz, G. Liva, E. Paolini, and M. Chiani, "Nonbinary protograph low-density parity-check codes for space communications," *Int. J. Satellite Commun. Netw.*, vol. 30, no. 2, pp. 43–51, Mar./Apr. 2012.

[24] Y. Wang, D. Liu, L. Sun, and S. Wu, "Real-time implementation for reduced-complexity LDPC decoder in satellite communication," *China Commun.*, vol. 11, no. 12, pp. 94–104, Dec. 2014.

[25] M. Baldi, N. Maturo, E. Paolini, and F. Chiaraluce, "On the use of ordered statistics decoders for low-density parity-check codes in space telecommand links," *J. Wirel. Commun.*, vol. 1, p. 272, May 2016.

[26] A. Morello and V. Mignone, "DVB-S2: The second generation standard for satellite broad-band services," *Proc. IEEE*, vol. 94, no. 1, pp. 210–227, Jan. 2006.

[27] S. Yuhai, L. Chunjiang, and Y. Ming, "The application of LDPC code in ABS-S system," in *Proc. IFITA*, Chengdu, China, May 2009, pp. 159–162.

[28] J. Su and Z. Lu, "Low cost VLSI design of the LDPC decoder in advanced broadcasting system for satellite," in *Proc. ICSICT*, Xi'an, China, Nov. 2012, pp. 1–3.

[29] J. Wen and X. Chang, "On the KZ Reduction," *IEEE Trans. Inf. Theory*, to be published.

[30] M. A. Aguirre, *Buy Introduction to Space Systems: Design and Synthesis* New York, NY, USA: Springer, 2013, pp. 378–380.

[31] L. J. Ippolito Jr, *Satellite Communications Systems Engineering: Atmospheric Effects, Satellite Link Design and System Performance*. West Sussex, U.K.: Wiley, 2017, pp. 316–324.

[32] C. C. Bassler, "Analysis and modeling of hydrodynamic components for ship roll motion in heavy weather," Ph.D. dissertation, Aerospace Eng., Virginia Polytechnic Inst. State Univ., Blacksburg, VA, USA, 2013.

[33] M. Anthony, *The Maritime Engineering Reference Book: A Guide to Ship Design, Construction and Operation* Oxford, U.K.: Butterworth-Heinemann Elsevier, 2008, pp. 7–9, pp. 505–507.

[34] E. C. Tupper, *Introduction to Naval Architecture*, 5th ed. Oxford, U.K.: Butterworth-Heinemann Elsevier, 2013, pp. 243–248.

[35] B. K. Henning, *Rules for Classification: Ships*. Oslo, Norway: DNV GL, Jul., 2017.

[36] T. I. Fossen, *Handbook of Marine Craft Hydrodynamics and Motion Control*. West Sussex, U.K.: Wiley, 2011, pp. 201–205.

[37] G. Maral, M. Bousquet, and Z. Sun, *Satellite Communications Systems: Systems, Techniques and Technology*, 5th ed. West Sussex, U.K.: Wiley, 2009, pp. 165–177.

[38] M. Imbert *et al.*, "Ku-band flat lens design for satellite TV applications," in *Proc. APSURSI*, Memphis, TN, USA, Apr. 2014, pp. 1453–1454.

[39] J. Tang, D. K. C. So, A. Shojaeifard, K.-K. Wong, and J. Wen, "Joint antenna selection and spatial switching for energy efficient MIMO SWIPT system," *IEEE Trans. Wireless Commun.*, vol. 16, no. 7, pp. 4754–4769, Jul. 2017.

[40] J. N. Pelton, S. Madry, and S. Camacho-Lara, *Handbook Satellite Application*, 2nd ed. Cham, Switzerland: Springer, 2017, pp. 511–514.

[41] J. Lee and K. A. S. Immink, "An efficient decoding strategy of 2D-ECC for optical recording systems," *IEEE Trans. Consum. Electron.*, vol. 55, no. 3, pp. 1360–1363, Aug. 2009.

[42] G. A. Malema, "Low-density parity-check codes: Construction and implementation," Ph.D. dissertation, Dept. Elect. Eng., Adelaide Univ., Adelaide, Australia, 2007.

BINGRUI WANG received the Ph.D. degree in microelectronics and solid state electronics from the Huazhong University of Science and Technology, China, in 2015. From 2017 to 2018, he was a Visiting Scholar with the Cluster of Science and Math, Singapore University of Technology and Design, Singapore. His primary research interests include error correction codes, field programmable gate array (FPGA) implementation, PCB design, and satellite communications.
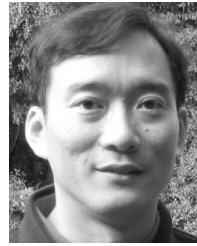
PINGPING CHEN (M'15) received the Ph.D. degree in electronic engineering from Xiamen University, China, in 2013. In 2012, he joined The Hong Kong Polytechnic University, Hong Kong, as a Research Assistant of electronic and information engineering. From 2013 to 2015, he was a Postdoctoral Fellow with the Institute of Network Coding, The Chinese University of Hong Kong, Hong Kong. He is currently a Professor with Fuzhou University, China. His primary research interests include channel coding, joint source and channel coding, network coding, and UWB communications.

YI FANG (M'15) received the Ph.D. degree in communication engineering from Xiamen University, China, in 2013. In 2012, he joined The Hong Kong Polytechnic University, Hong Kong, as a Research Assistant of electronic and information engineering. From 2012 to 2013, he was a Visiting Scholar of electronic and electrical engineering with University College London, U.K. From 2014 to 2015, he was a Research Fellow with the School of Electrical and Electronic Engineering, Nanyang Technological University, Singapore. He is currently an Associate Professor with the School of Information Engineering, Guangdong University of Technology. His current research interests include information and coding theory, low-density parity check (LDPC)/protograph codes, spread-spectrum modulation, and cooperative communications.

FRANCIS C. M. LAU (M'93–SM'03) received the B.Eng. degree (Hons.) in electrical and electronic engineering from the King's College London and the Ph.D. degree from the University of London, U.K. He is currently a Professor and an Associate Head of the Department of Electronic and Information Engineering, The Hong Kong Polytechnic University, Hong Kong. He has coauthored *Chaos-Based Digital Communication Systems* (Heidelberg: Springer-Verlag, 2003) and *Digital Communications with Chaos: Multiple Access Techniques and Performance Evaluation* (Oxford: Elsevier, 2007). He is also a co-holder of five U.S. patents. He has published around 300 papers. His main research interests include channel coding, cooperative networks, wireless sensor networks, chaos-based digital communications, applications of complex-network theories, and wireless communications. He is also a Fellow of the IET. He was the Chair of the Technical Committee on Nonlinear Circuits and Systems, IEEE Circuits and Systems Society, from 2012 to 2013. He also serves as a General Co-Chair for the International Symposium on Turbo Codes and Iterative Information Processing 2018. He served as an Associate Editor for the IEEE TRANSACTIONS ON CIRCUITS AND SYSTEMS II, from 2004 to 2005, the IEEE TRANSACTIONS ON CIRCUITS AND SYSTEMS I, from 2006 to 2007, and *IEEE Circuits and Systems Magazine*, from 2012 to 2015. He has been a Guest Associate Editor of the *International Journal and Bifurcation and Chaos*, since 2010, and an Associate Editor of the IEEE TRANSACTIONS ON CIRCUITS AND SYSTEMS II, since 2016.

• • •